

# Constructing meaningful FWI gradients from DAS data

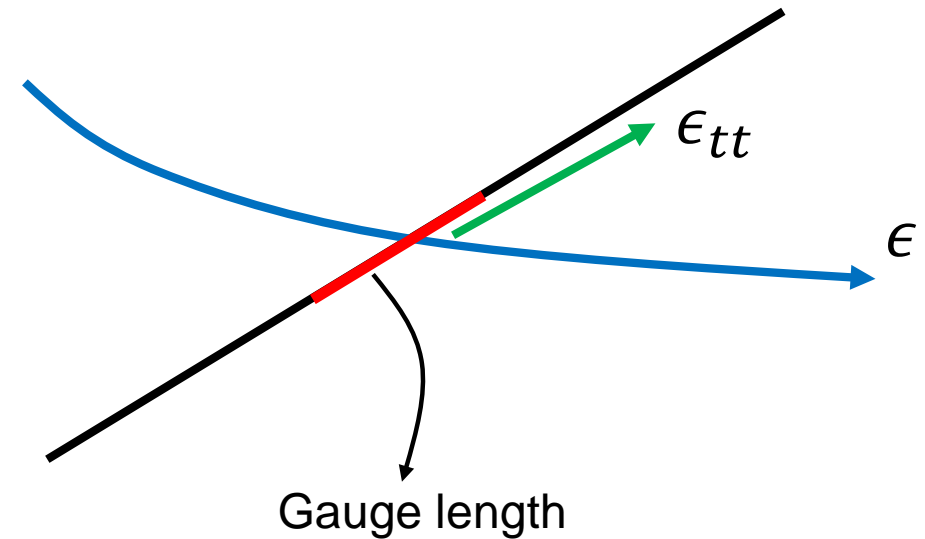
Matt Eaid\*, Scott Keating, and Kris Innanen

CREWES Sponsors Meeting, Banff,  
December 11<sup>th</sup>, 2019



- Growing interest in the use of DAS fibres for seismic acquisition.
- Need to develop strategies for including the data they provide in FWI.
- Geophones and DAS provide complementary datasets.

- DAS uses an optical fibre to make measurements of seismic strain
- Fibres are only sensitive to strain along the tangent of the fibre
- Measurements are spatially averaged over the gauge length to improve SNR





# Full waveform inversion

Receiver matrix

Observed data

$$\phi = \frac{1}{2} \|\mathbf{R}\mathbf{u} - \mathbf{d}\|_2^2$$

Modeled wavefield

Forward wavefield propagation

$$\mathbf{S}\mathbf{u} = \mathbf{f}$$

$$\frac{\partial \phi}{\partial \mathbf{m}} = \left\langle \frac{\partial S}{\partial \mathbf{m}} \mathbf{u}, \lambda \right\rangle$$

Forward propagated wavefield

Back-propagated adjoint wavefield

Reverse wavefield propagation

$$\mathbf{S}^\dagger \lambda = \mathbf{R}^\mathbf{T} (\mathbf{R}\mathbf{u} - \mathbf{d})$$



# Full waveform inversion

Receiver matrix

Observed data

$$\phi = \frac{1}{2} \|\mathbf{R}\mathbf{u} - \mathbf{d}\|_2^2$$

Modeled wavefield

Forward wavefield propagation

$$\mathbf{S}\mathbf{u} = \mathbf{f}$$

$$\frac{\partial \phi}{\partial \mathbf{m}} = \left\langle \frac{\partial S}{\partial \mathbf{m}} \mathbf{u}, \lambda \right\rangle$$

Forward propagated wavefield

Back-propagated adjoint wavefield

Reverse wavefield propagation

$$\mathbf{S}^\dagger \lambda = \mathbf{R}^\mathbf{T} (\mathbf{R}\mathbf{u} - \mathbf{d})$$



# Receiver Matrix (R)

## Geophones

- Samples displacement wavefield at location of geophones

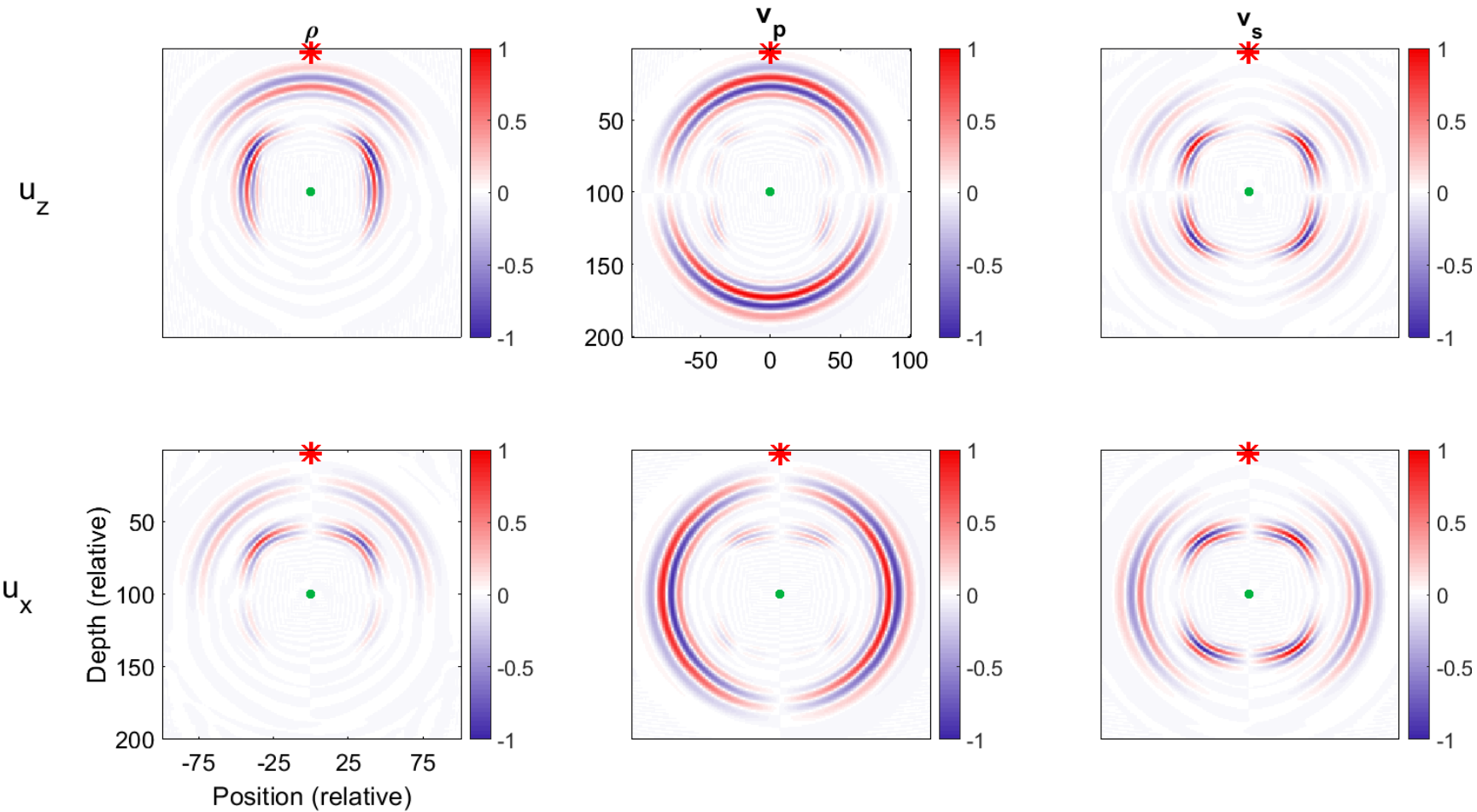
## DAS

- Computes strain from displacement wavefields.
- Computes fibre strain, using fibre geometry.
- Invokes gauge length averaging of fibre sensitivity.

$$\begin{array}{c}
 \begin{bmatrix} d'_1 \\ d'_2 \\ d'_3 \\ d'_4 \\ \vdots \\ d'_{N_R-1} \\ d'_{N_R} \end{bmatrix} \\
 (N_R \times 1)
 \end{array}
 =
 \begin{array}{c}
 \begin{bmatrix} u_{m_x}^1 \\ u_{m_z}^1 \\ u_{m_x}^2 \\ u_{m_z}^2 \\ \vdots \\ u_{m_x}^{N_{g_x}} \\ u_{m_z}^{N_{g_z}} \end{bmatrix} \\
 (2N_g \times 1)
 \end{array}
 \begin{array}{c}
 R \\
 (N_R \times 2N_g)
 \end{array}
 \\
 \\
 \begin{array}{c}
 \begin{bmatrix} d_{m_x}^1 \\ d_{m_z}^1 \\ d_{m_x}^2 \\ d_{m_z}^2 \\ \vdots \\ d_{m_x}^{N_{R_x}} \\ d_{m_z}^{N_{R_z}} \\ \hline d'_1 \\ d'_2 \\ d'_3 \\ d'_4 \\ \vdots \\ d'_{N_R-1} \\ d'_{N_R} \end{bmatrix} \\
 (N_R \times 1)
 \end{array}
 =
 \begin{array}{c}
 \begin{bmatrix} R_{GEO} \\ \hline R_{DAS} \end{bmatrix} \\
 (N_R \times 2N_g)
 \end{array}
 \begin{array}{c}
 \begin{bmatrix} u_{m_x}^1 \\ u_{m_z}^1 \\ u_{m_x}^2 \\ u_{m_z}^2 \\ \vdots \\ u_{m_x}^{N_{g_x}} \\ u_{m_z}^{N_{g_z}} \end{bmatrix} \\
 (2N_g \times 1)
 \end{array}
 \end{array}$$



# Scattering Radiation Patterns: Displacement

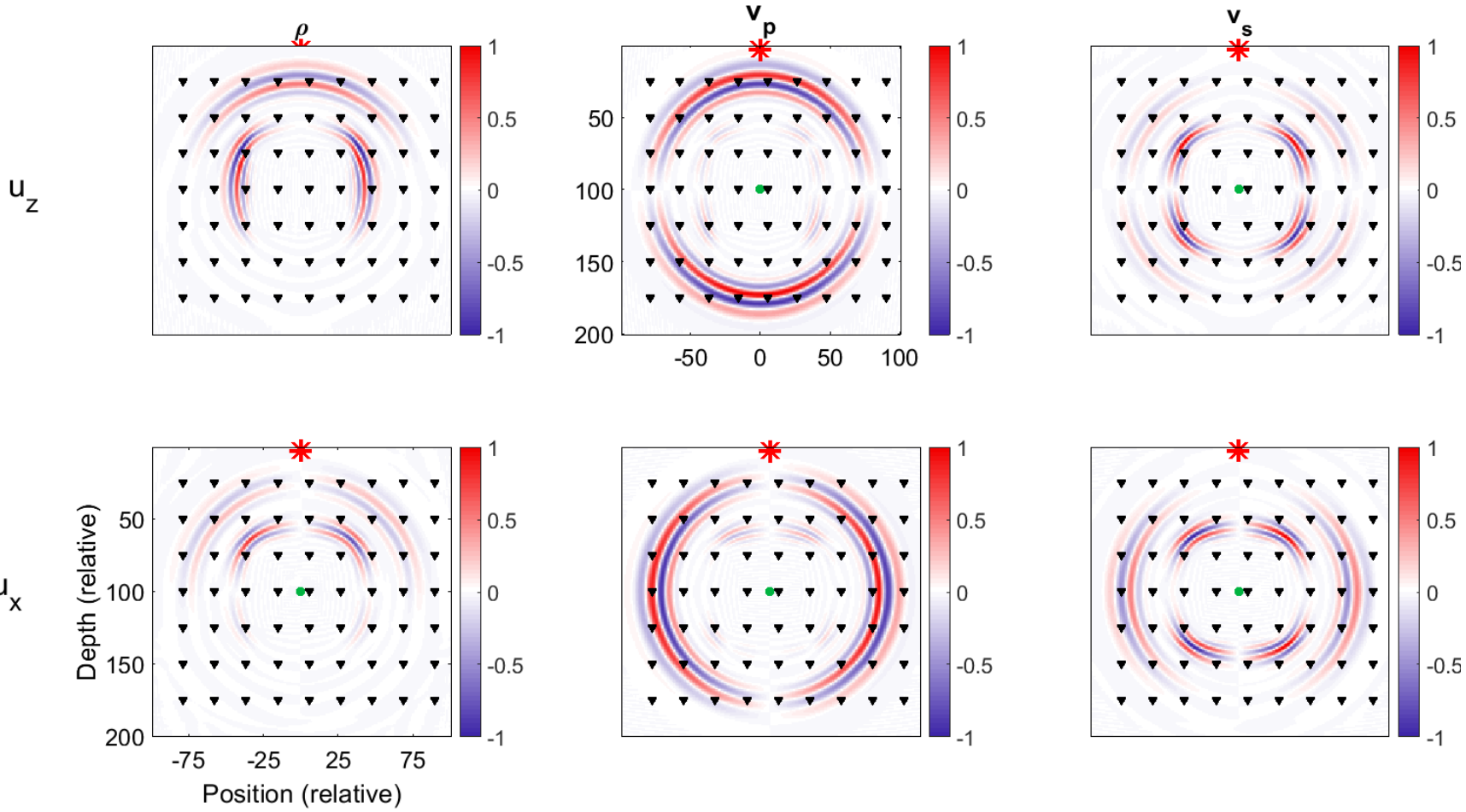


Scattering radiation patterns provide insight into the sensitivity of the wavefield to perturbations in certain model parameters.

$$\frac{\partial \mathbf{u}}{\partial \mathbf{m}} \approx \mathbf{u}_p - \mathbf{u}_r$$



# Scattering Radiation Patterns: Displacement



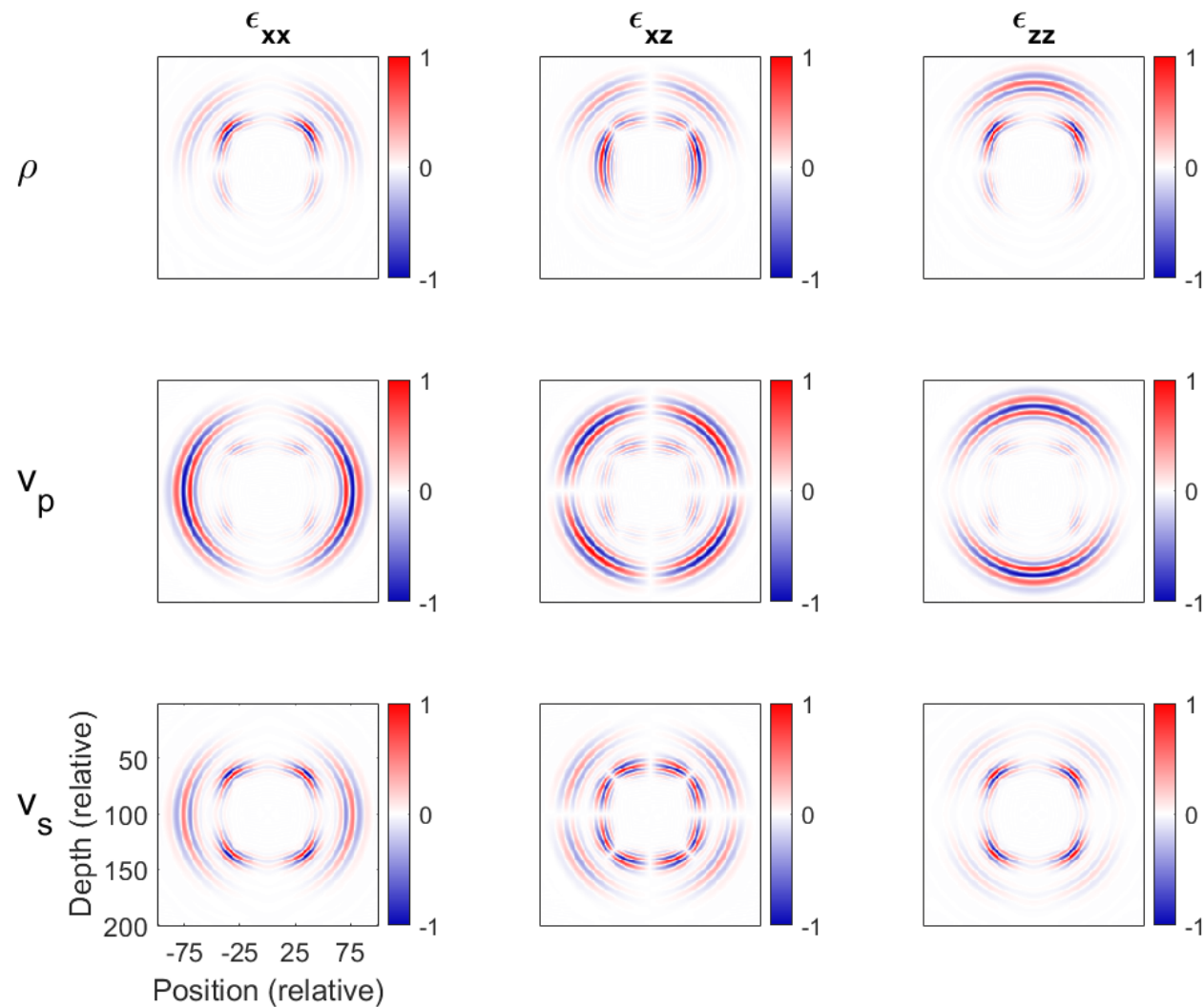
Scattering radiation patterns provide insight into the sensitivity of the wavefield to perturbations in certain model parameters.

$$\frac{\partial \mathbf{u}}{\partial \mathbf{m}} \approx \mathbf{u}_p - \mathbf{u}_r$$





# Scattering Radiation Patterns: Strain

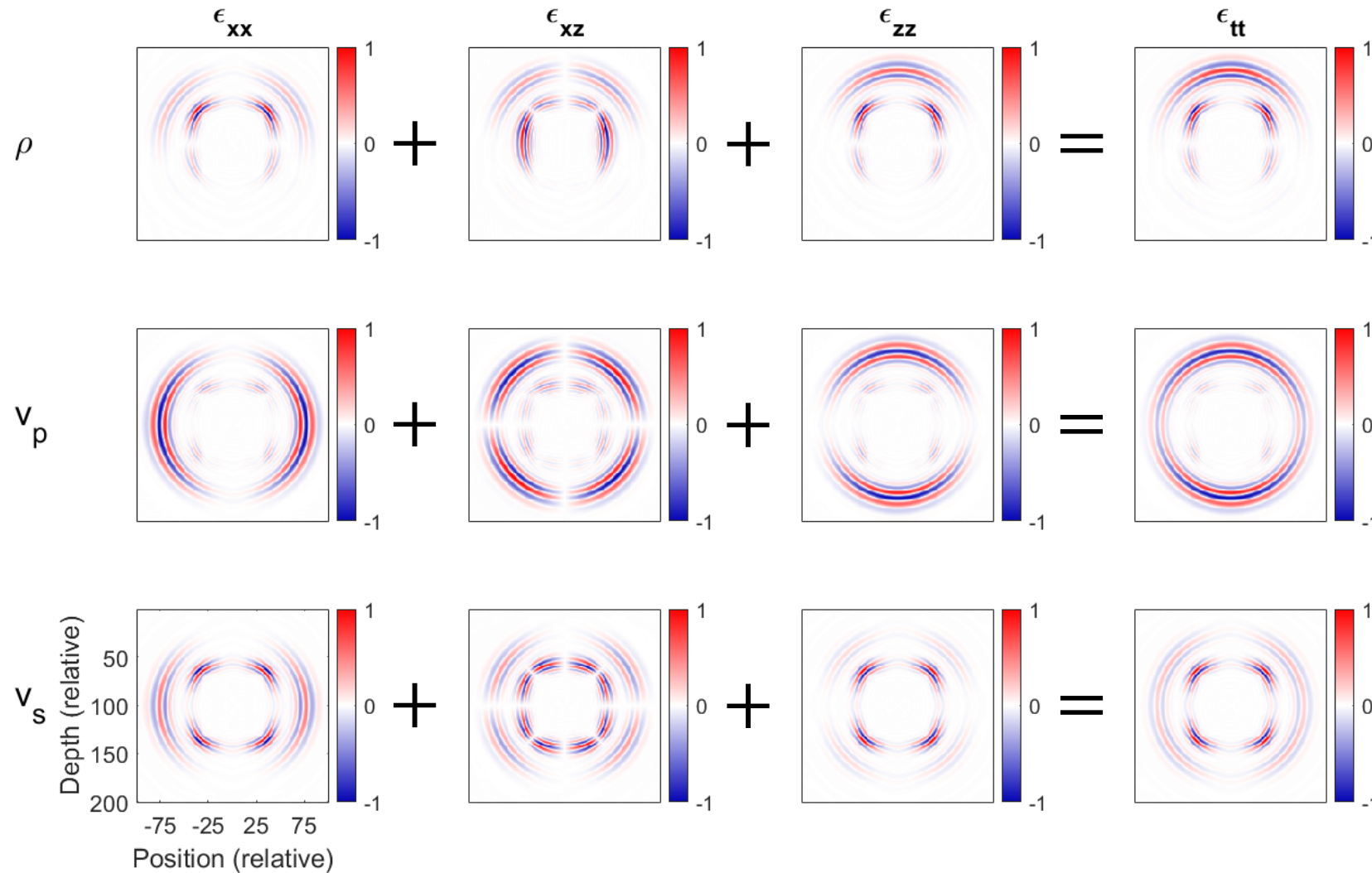


Strain radiation patterns provide insight into the sensitivity of the strain field to model perturbations.

$$\epsilon_{ij} = \frac{1}{2} \left( \frac{u_i}{x_j} + \frac{u_j}{x_i} \right)$$



# Scattering Radiation Patterns: Strain



Strain radiation patterns provide insight into the sensitivity of the strain field to model perturbations.

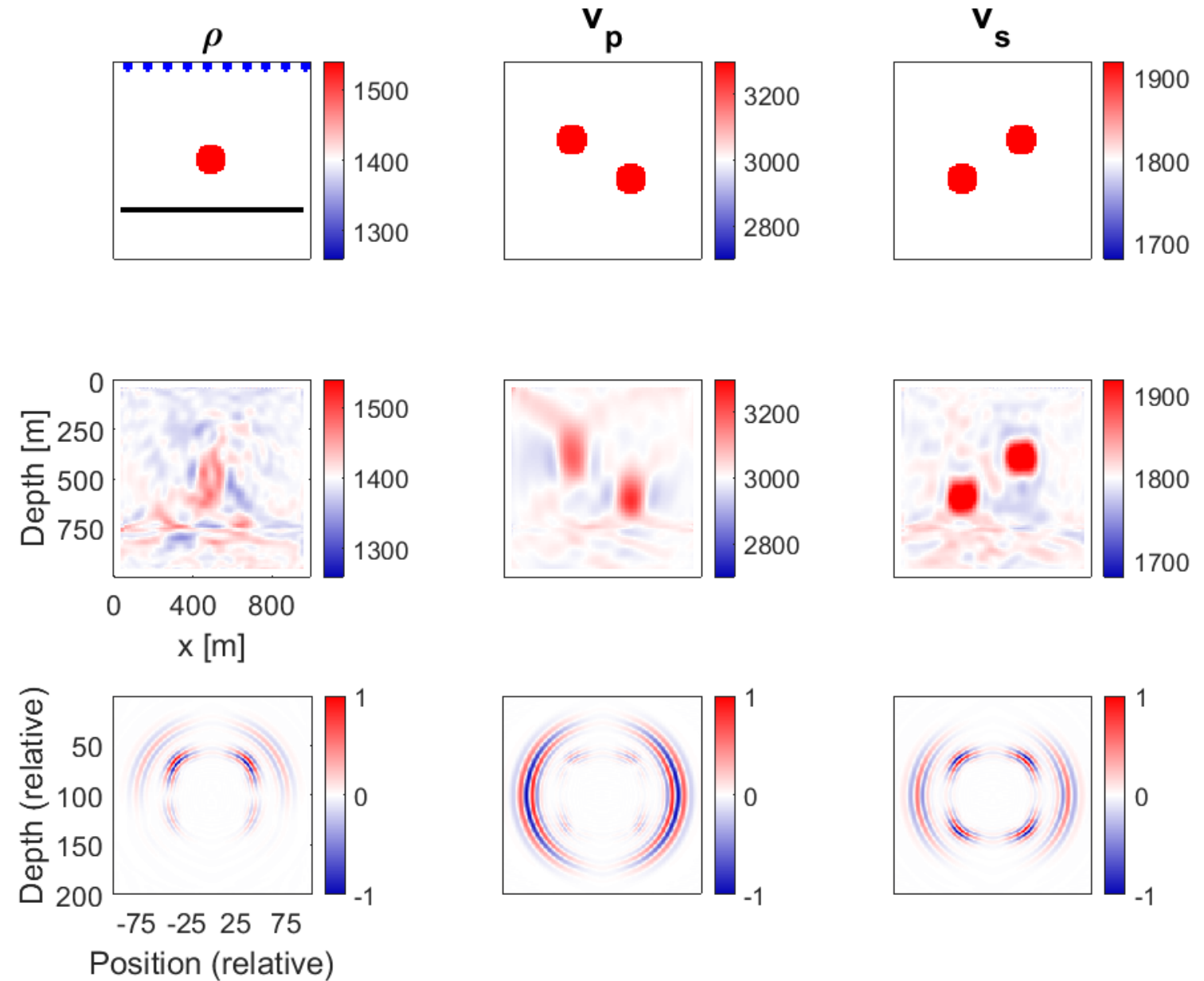
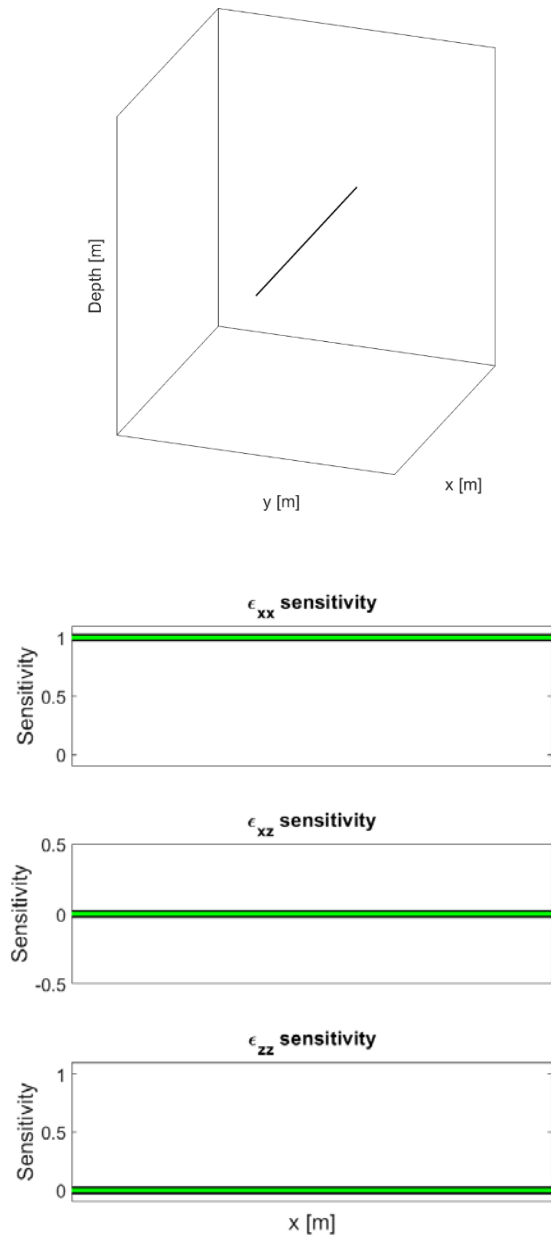
$$\epsilon_{ij} = \frac{1}{2} \left( \frac{u_i}{x_j} + \frac{u_j}{x_i} \right)$$

The fibre sensitive radiation patterns are formed through a weighted sum of the strain radiation patterns.

$$\epsilon_{tt} = a^2 \epsilon_{xx} + 2b \epsilon_{xz} + c^2 \epsilon_{zz}$$

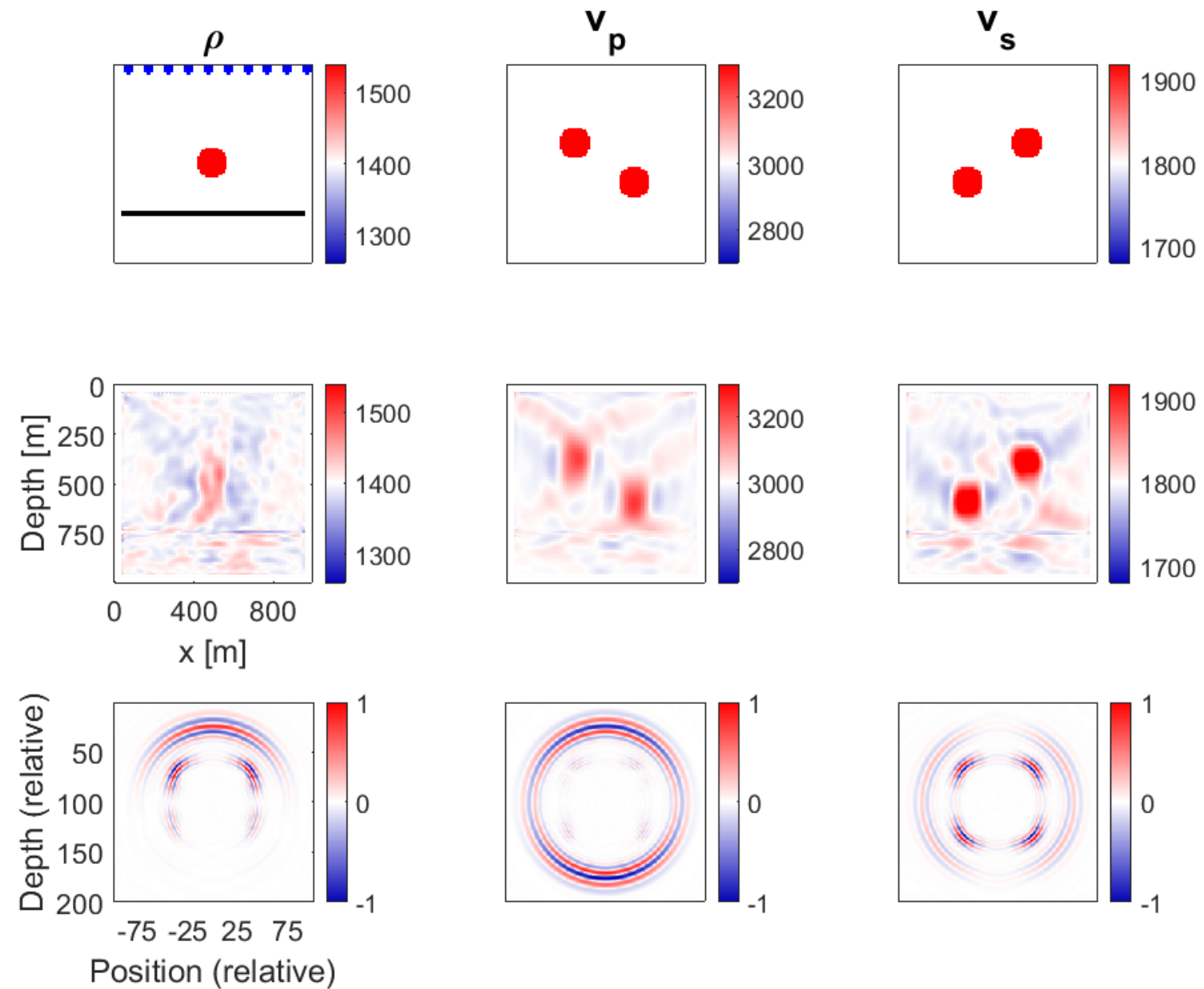
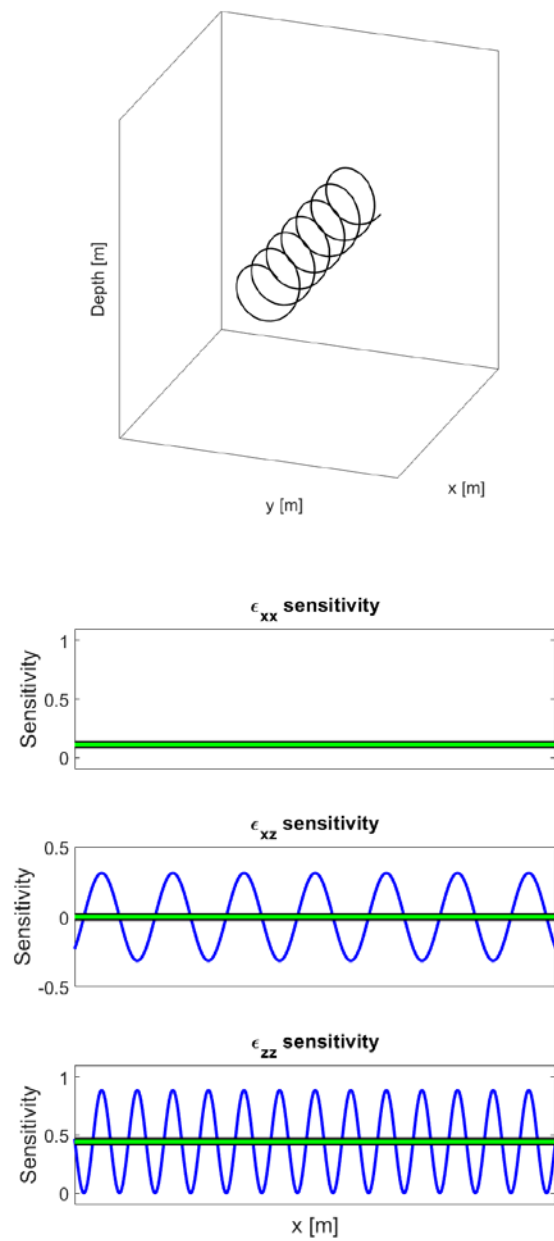


# Toy Model: DAS data inversion, straight fibre



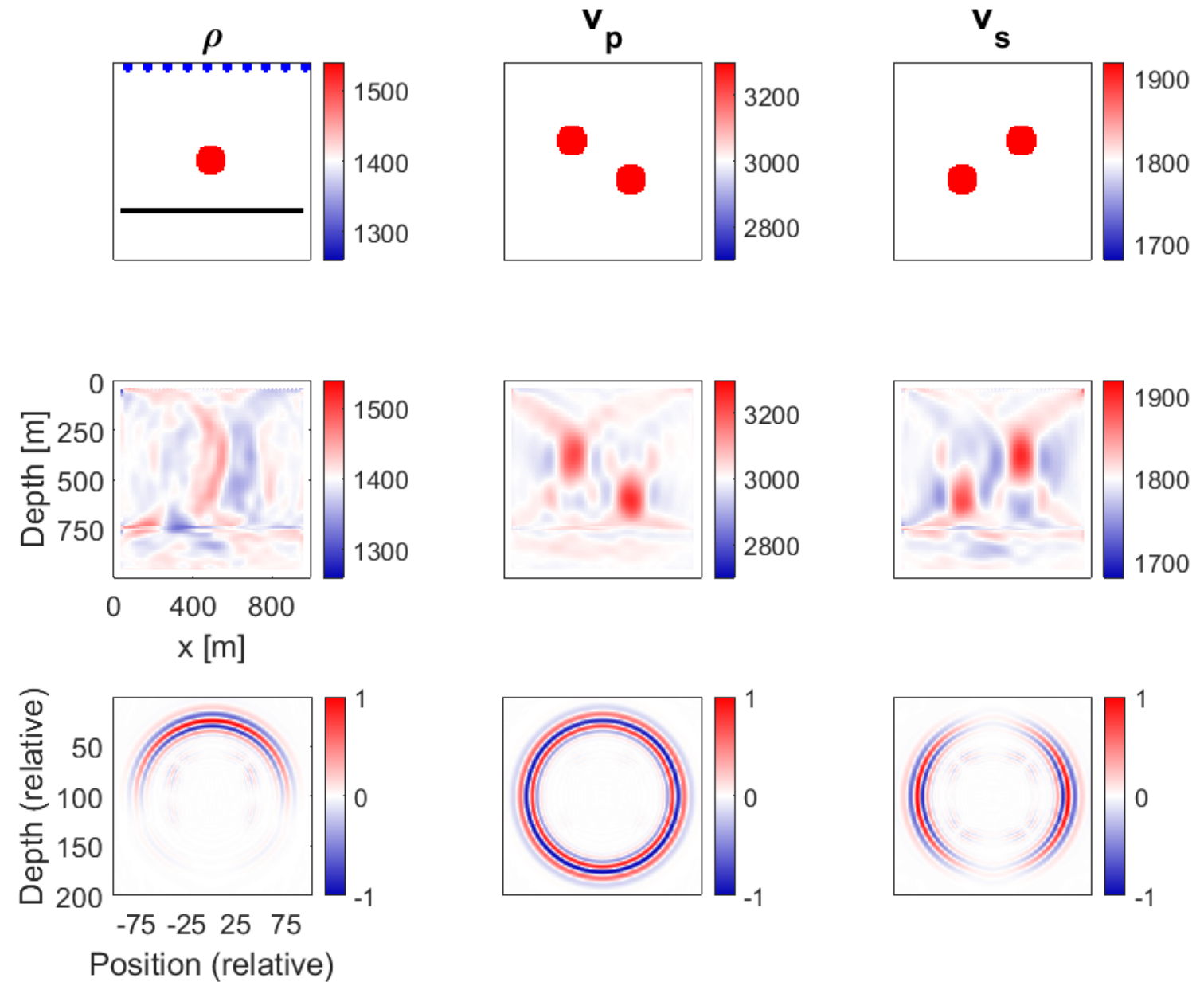
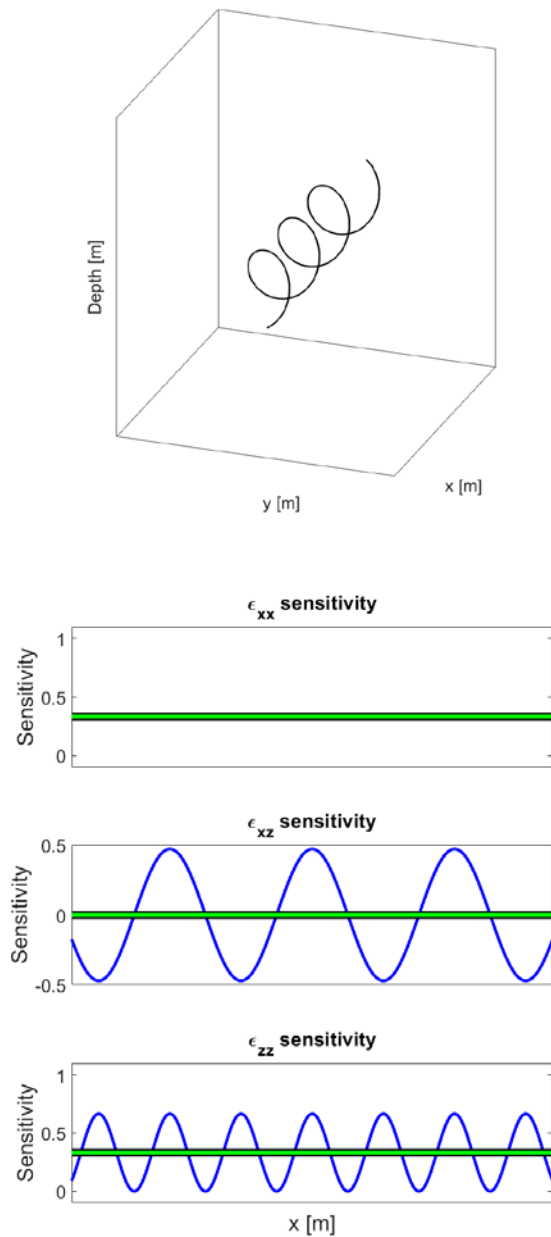


# Toy Model: DAS data inversion, 19 degree lead angle (1:4)



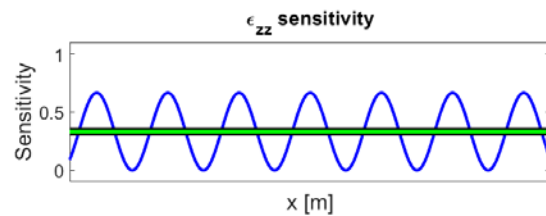
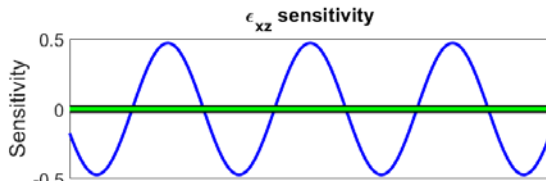
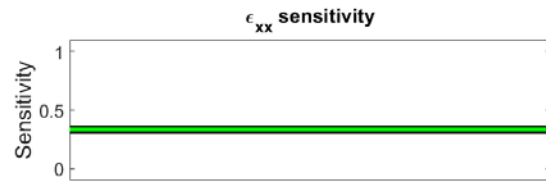
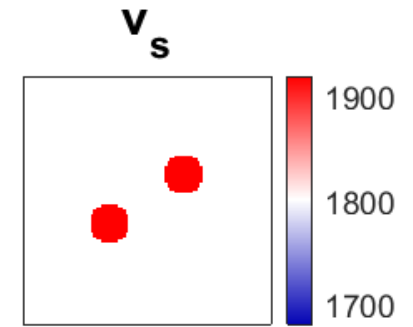
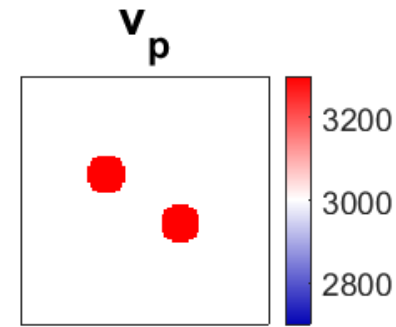
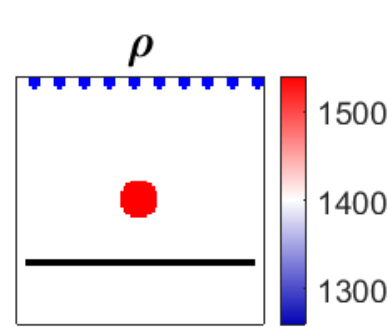
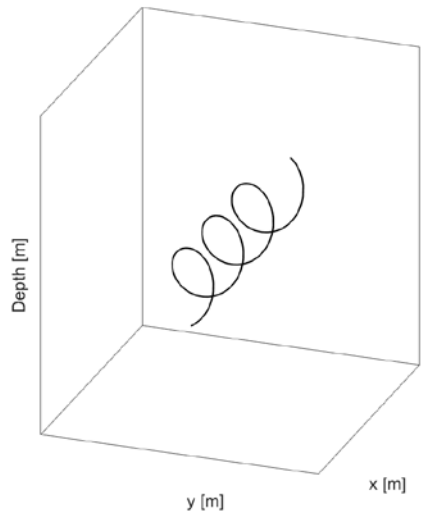


# Toy Model: DAS data inversion, 35 degree lead angle (1:1)

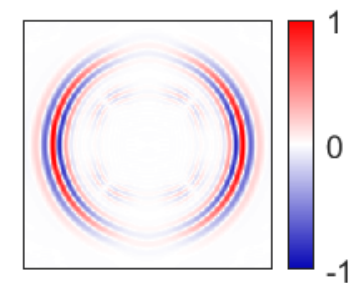
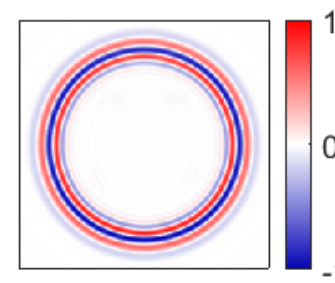
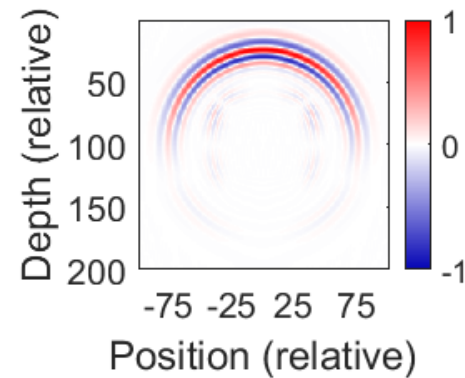




# Toy Model: DAS data inversion, 35 degree lead angle (1:1)

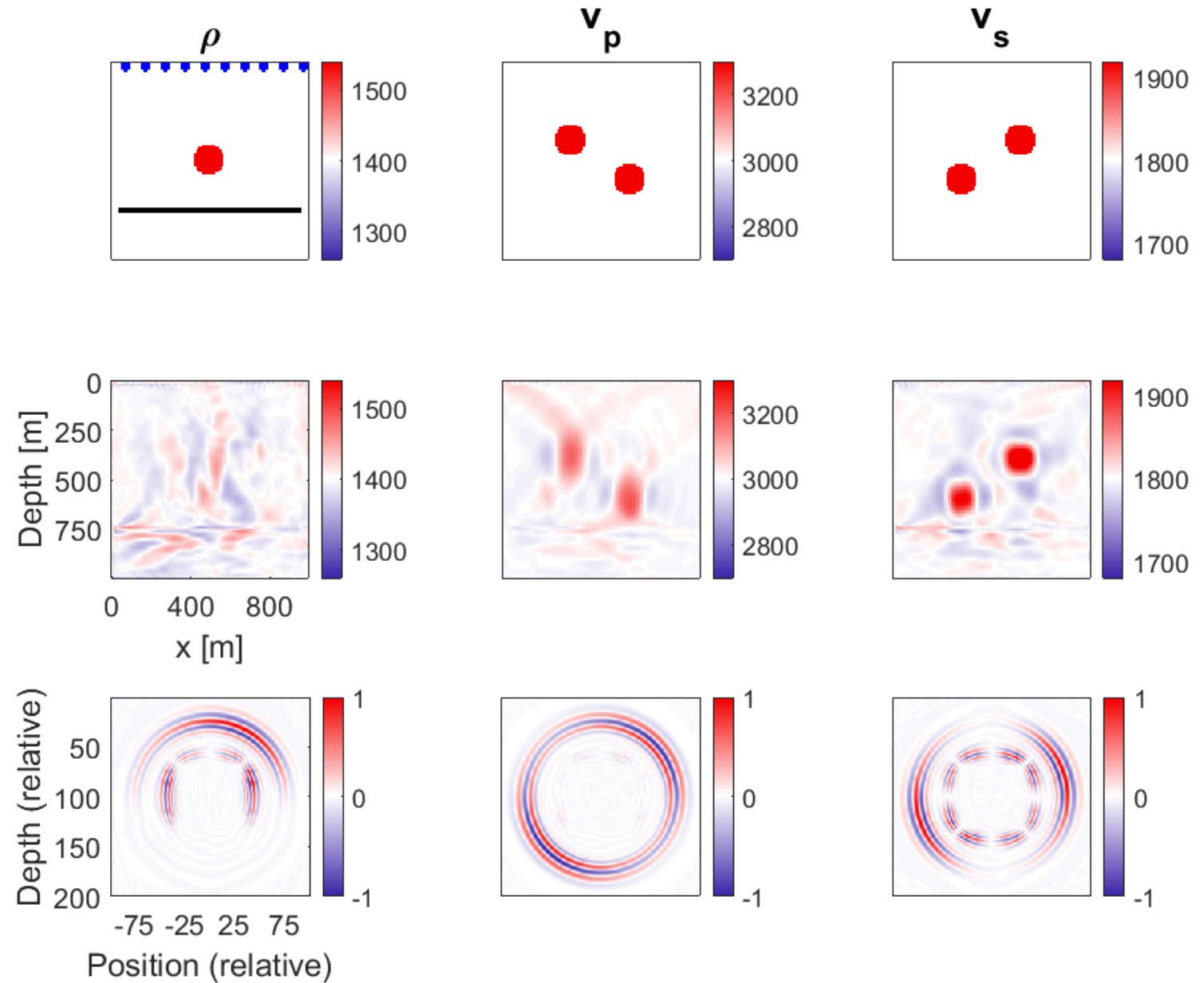
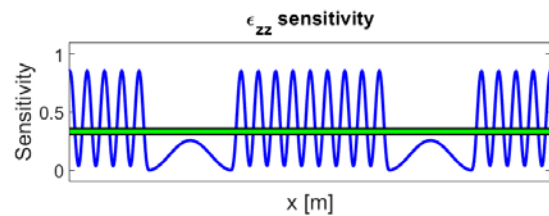
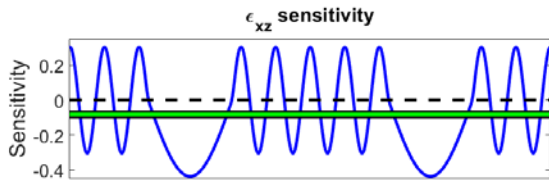
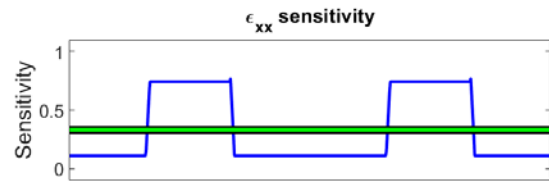
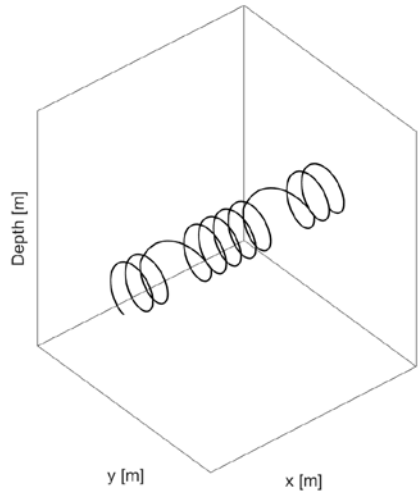


$$\epsilon_{tt} = 1\epsilon_{xx} + 1\epsilon_{zz} = \frac{\partial u_x}{\partial x} + \frac{\partial u_z}{\partial z} = \nabla \cdot u$$





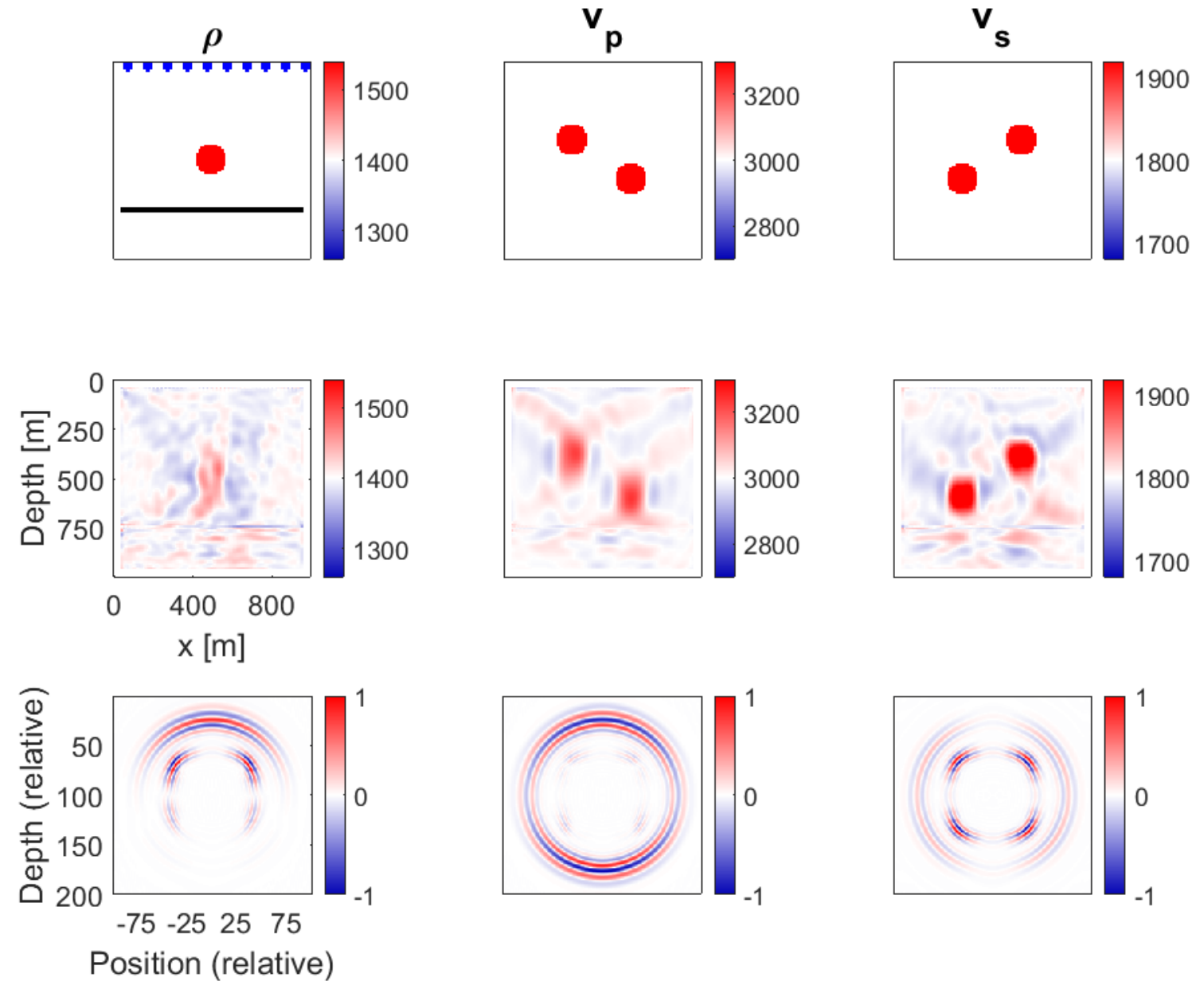
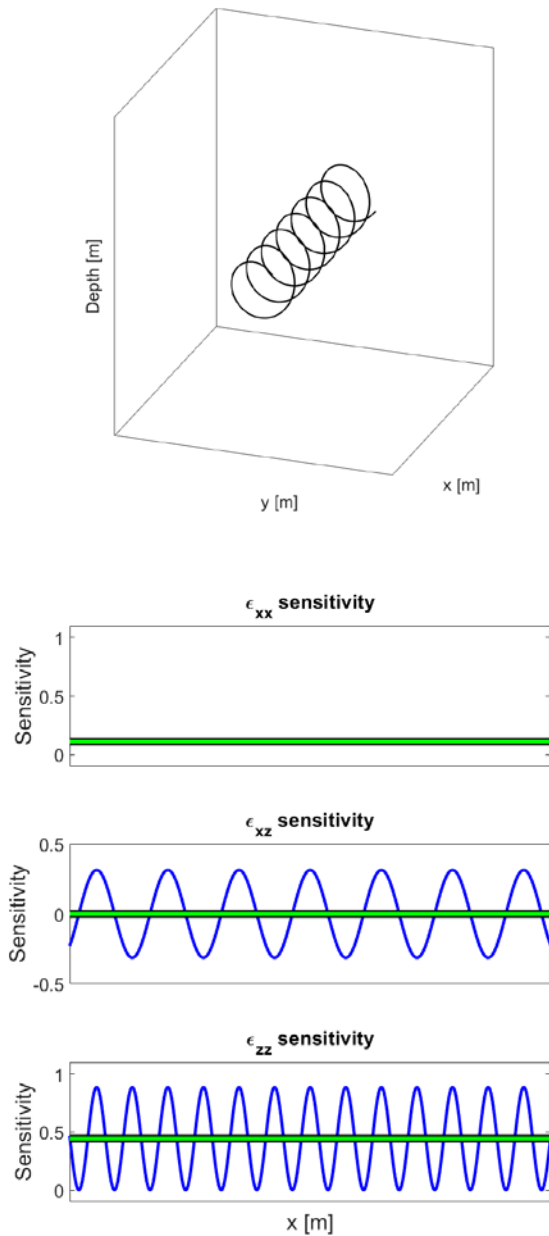
# Toy Model: DAS data inversion, asymmetric fibre (2:1:2)







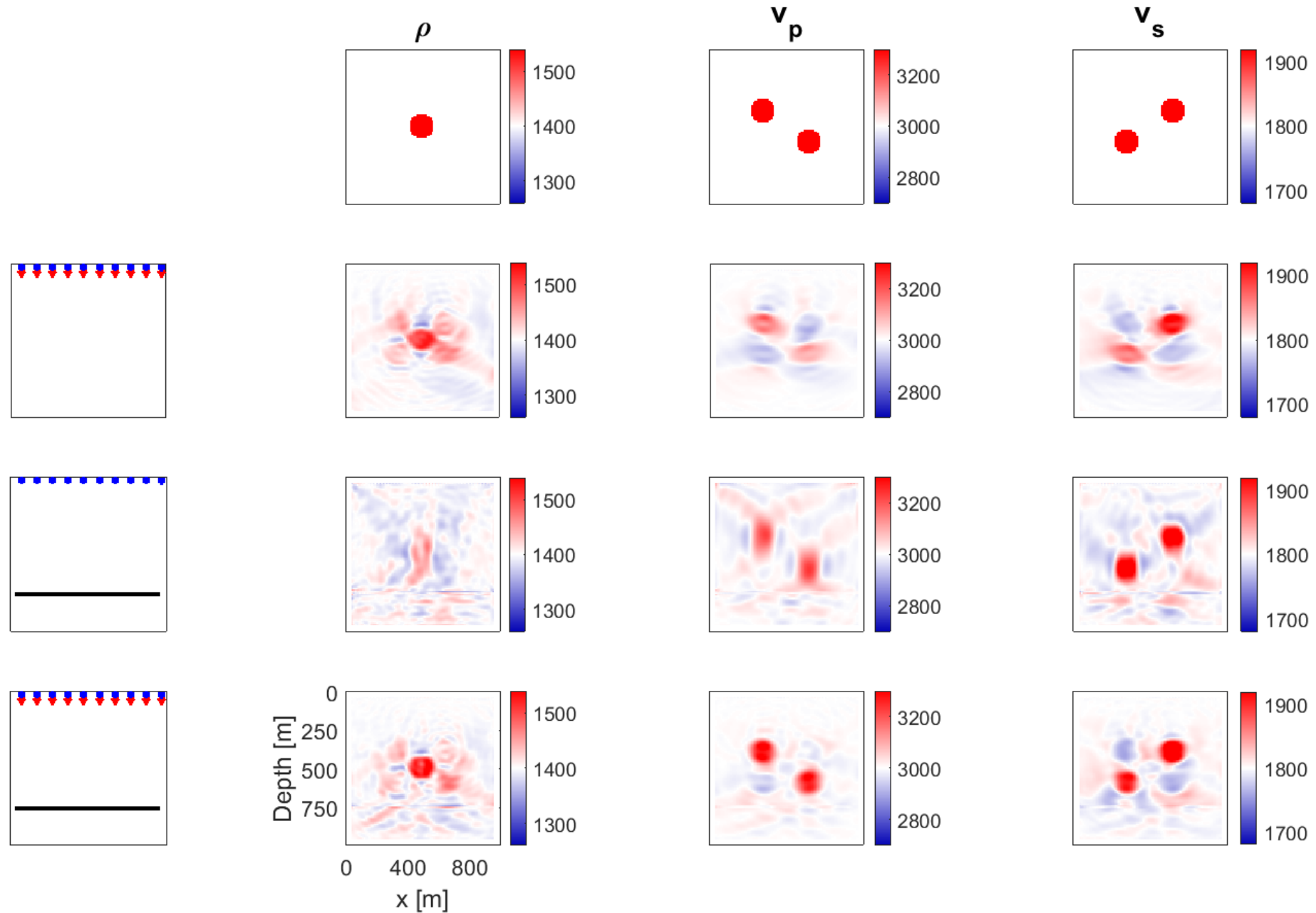
# Toy Model: DAS data inversion, 19 degree lead angle (1:4)





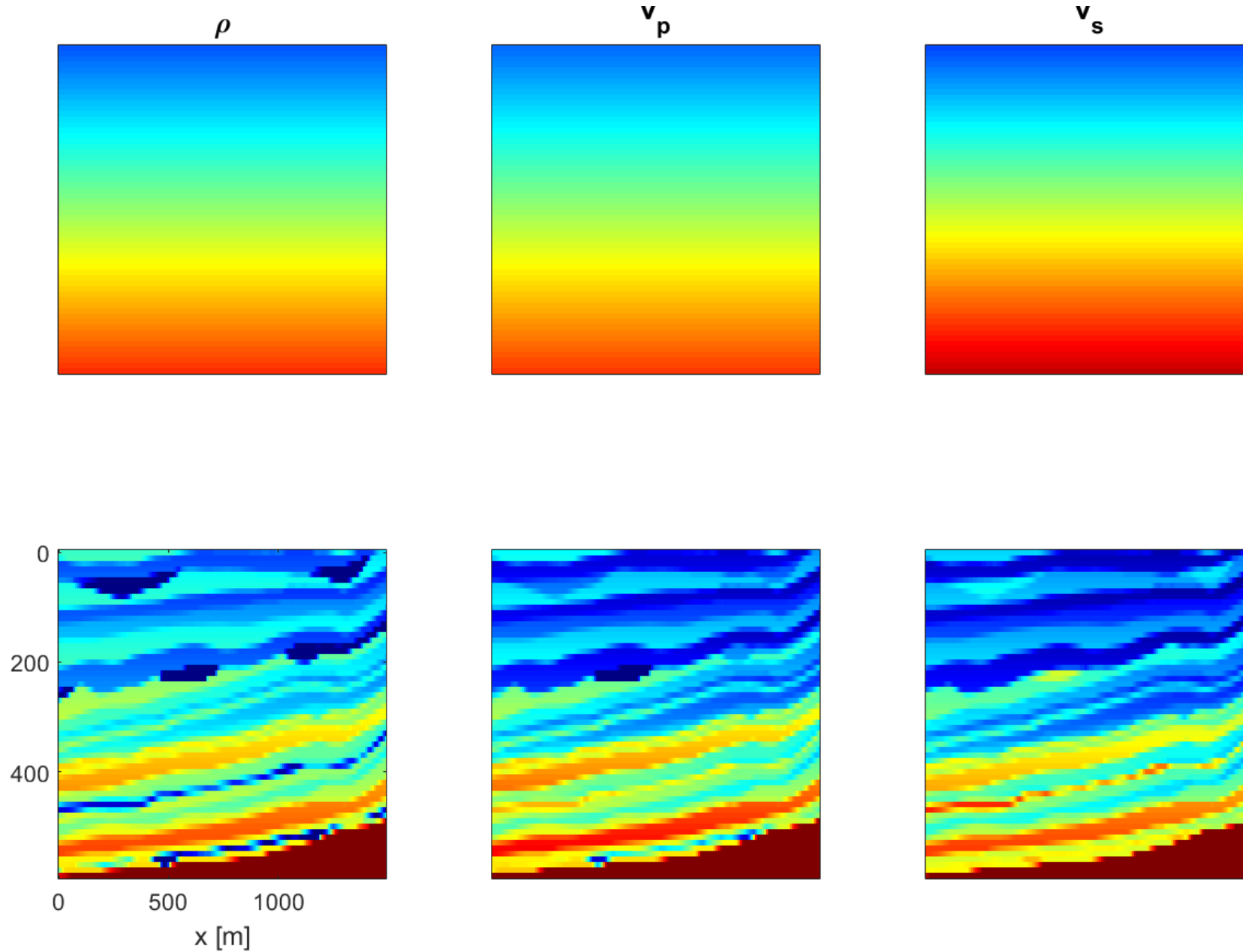


# Toy Model: Geophone and DAS Simultaneous Inversion



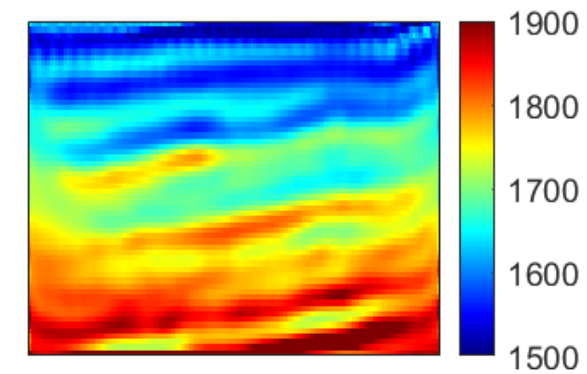
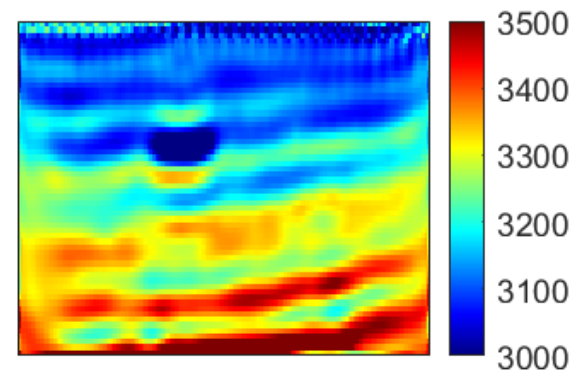
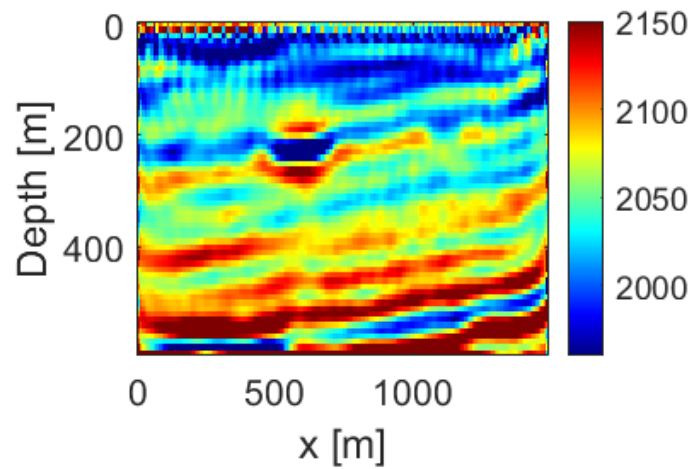
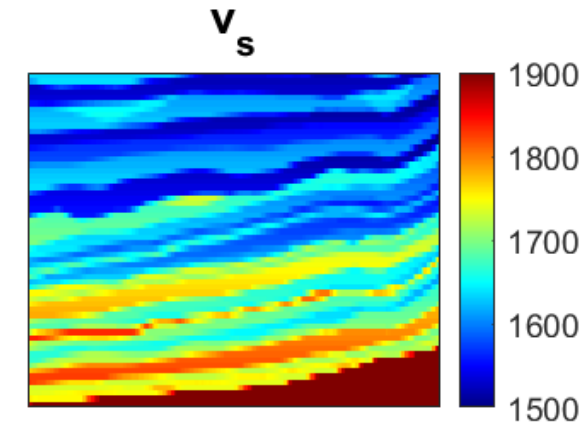
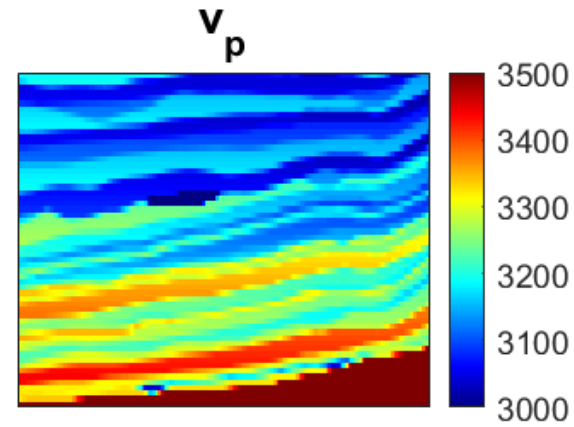
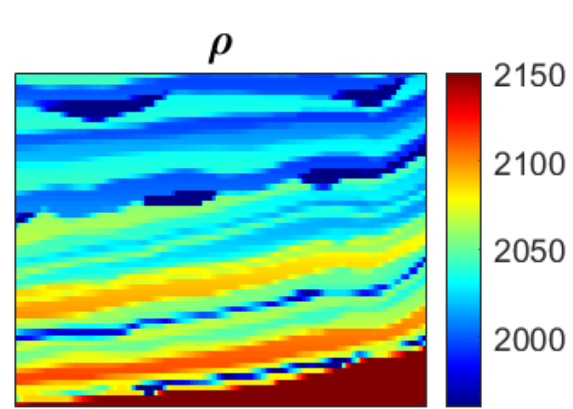


# Marmousi 2 Models



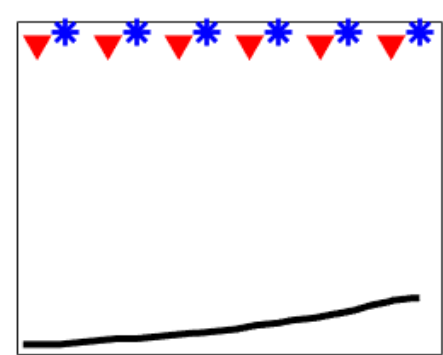
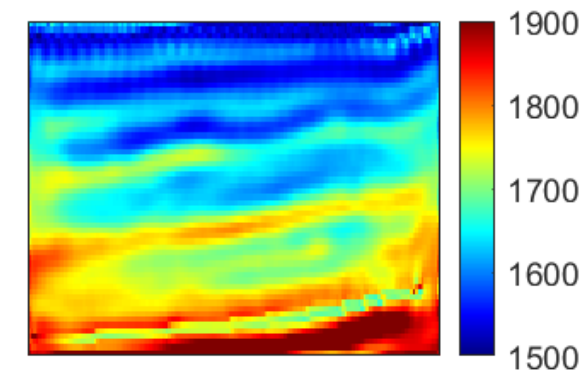
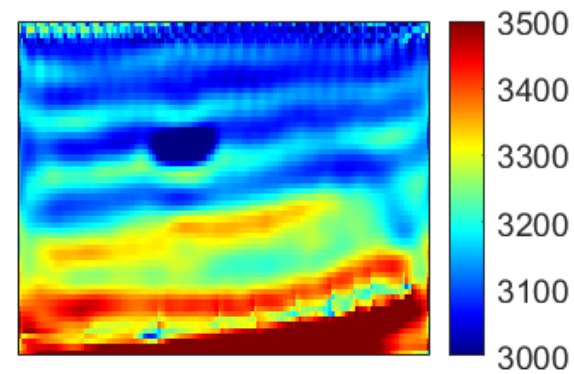
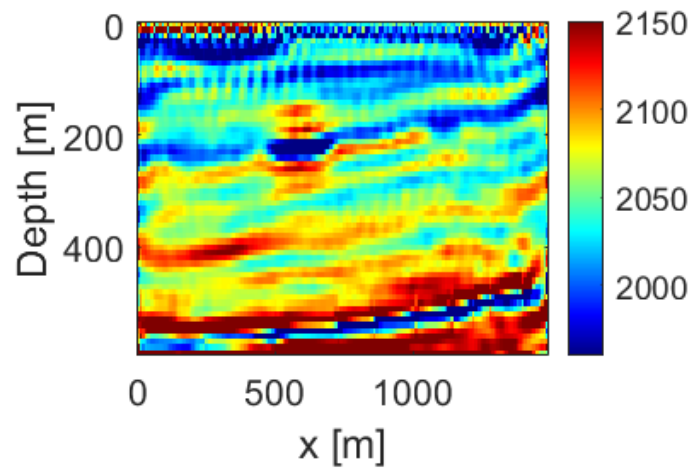
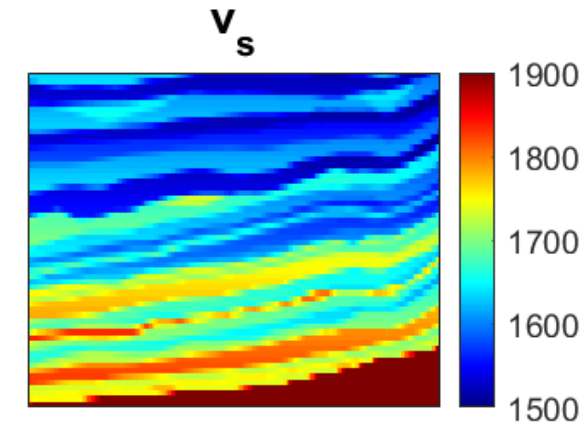
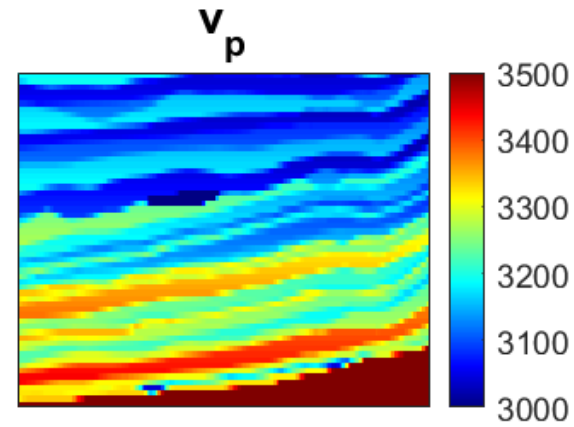
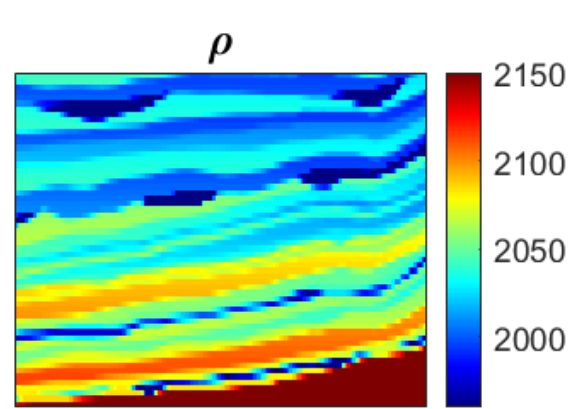


# Marmousi 2: geophone data inversion





# Marmousi 2: simultaneous geophone and DAS data inversion





- DAS data can be readily accommodated in standard FWI algorithms by redefining  $R$ .
- Varying the fibre geometry greatly alters their sensitivity and ability to estimate parameters.
- DAS and geophones can provide complementary information that results in improved parameter estimations.



- CREWES Industrial Sponsors
- NSERC (CRDPJ 461179-13)
- SEG Foundation
- CREWES Staff and Students